

Generation of tunable mid-infrared picosecond pulses at 76 MHz

A. G. Yodh,* H. W. K. Tom, G. D. Aumiller, and R. S. Miranda

AT&T Bell Laboratories, Holmdel, New Jersey 07733

Received December 5, 1990; revised manuscript received February 21, 1991

We describe and characterize an experimental apparatus that generates tunable infrared light pulses from 3.4 to 7.0 μm by difference-frequency mixing in AgGaS_2 . The pulses are 2.16 ps in duration, have a frequency bandwidth of 6.6 cm^{-1} , and are produced at a 76-MHz repetition rate. Because the apparatus is compatible with low signal lock-in modulation and signal-averaging techniques, the infrared probe pulses can be used to measure very small ($<10^{-4}$) vibrational absorption changes on fast time scales. We demonstrate this sensitivity by using the source to perform linear vibrational spectroscopy of adsorbed CO on Cu[111].

Infrared (IR) spectroscopy has proved to be an extremely valuable tool for the identification of different chemical species, the study of chemical bonding, the study of narrow bandgap semiconductors, and the observation of midgap excitations in semiconductors. At present some of the most interesting physical questions in these systems are concerned with intramolecular and intermolecular dynamical processes such as energy transfer and dephasing phenomena.¹ In the investigation of these fast processes, tunable, ultrashort pulses in the mid-IR frequency range are highly desirable. Existing laser systems in this spectral region are limited, however. To circumvent these limitations, several laser-based tunable picosecond-subpicosecond light sources have been developed.²⁻¹⁰ All these systems incorporate some form of nonlinear-optical wave mixing. In the present paper we describe an apparatus that can be used to carry out picosecond time-resolved spectroscopy in the mid-IR spectral region. The apparatus, which is easily constructed with standard optical components, is compatible with low signal lock-in modulation and signal-averaging schemes and can be used to observe signal variation at the level of 10^{-6} . As a first step toward these types of study we demonstrate that the source can be used to perform linear vibrational absorption measurements of molecular CO adsorbed on Cu[111].

We have produced 2.16-ps pulses of IR radiation that are tunable from 3.4 to 7.0 μm by difference-frequency mixing in AgGaS_2 .¹¹ In contrast to IR sources based on mixing in LiNbO_3 ,^{3,5,6} AgGaS_2 (Refs. 12 and 13) has the spectral transparency, phase matchability, and crystal quality to permit tuning well beyond 5 μm and therefore makes possible studies of a wider range of molecular vibrations and narrow-bandgap semiconductors. Recent studies that used AgGaS_2 to generate 8-ps IR pulses in the same frequency range were based on low-repetition-rate, high-power amplified Nd:YAG/glass laser systems.^{2,4} In addition, IR pulses as short as 100 fs have now been derived from amplified colliding pulse mode-locked (CPM) systems operating at 8 kHz.¹⁴ These approaches are well suited to saturation and recovery pump-probe studies in which peak signal changes are greater than 10%. Our source is derived from a cw mode-locked Nd:YAG laser at

a 76-MHz repetition rate. It is brighter than the lower-repetition-rate systems and, as is discussed above, is particularly well suited to pulling small signals out of large backgrounds. We note that some early investigations of the generation of IR pulses based on mode-locked argon-ion lasers were carried out¹⁵ and that a similar high-repetition-rate system, capable of tuning to 4 μm with KTiOPO_4 as the mixing crystal, was recently reported.¹⁶

In addition to the studies cited above, other schemes designed to generate tunable mid-IR radiation, such as stimulated electronic Raman scattering in alkali vapors^{7,8,17} and parametric conversion processes,¹⁸ have been investigated. In some instances these schemes have been useful, but typically they also require large pump energies and operate at low repetition rates.

EXPERIMENT

The heart of our high-repetition-rate system (see Fig. 1) is a cw mode-locked Nd:YAG laser that produces 90-ps, 1.06- μm pulses at a 76-MHz repetition rate. 10 W of average power at 1.06 μm is frequency doubled with a KTP crystal, producing ~ 1 W of 0.532- μm radiation. The frequency-doubled light is used for synchronous pumping of a dye laser that uses LDS 867 and LDS 821 dyes and has a three-plate birefringent filter. The dye laser emits a train of 3-ps (intensity FWHM) pulses that are tunable from 810 to 960 nm. The remaining 1.06- μm light (that which is not upconverted in the KTP crystal) is compressed to 3.75 ps (FWHM) with a standard fiber-grating configuration.¹⁹ Approximately 470 mW of horizontally polarized compressed 1.06- μm radiation and 50 mW of vertically polarized dye laser output are mixed in type I phase-matched ($e = o + o$ for $\omega_{\text{dye}} = \omega_{1.06} + \omega_{\text{IR}}$) AgGaS_2 to generate ~ 16.5 μW of IR radiation (for $\lambda_{\text{IR}} = 5$ μm). The input beams are made time coincident with a delay line and collinear with a beam-splitting polarizer. The AgGaS_2 crystal (Cleveland Crystals) was 1.65 mm long and was cut at 53.2° with respect to the optic axis. The two input beams were focused to $\omega_0 = 60$ μm spots [assuming a Gaussian intensity profile $I(r) = \exp(-2r^2/\omega_0^2)$] in the crystal. We assume that the IR generation had a waist

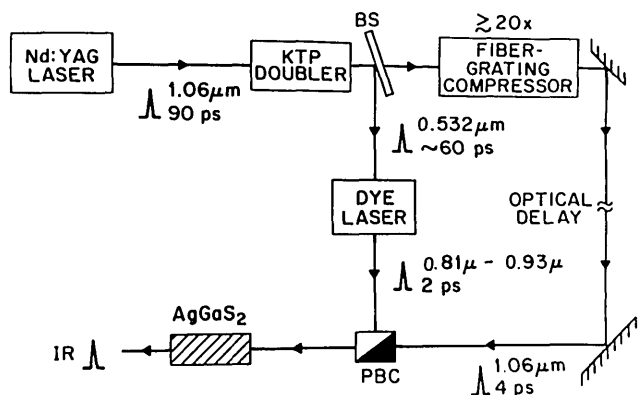


Fig. 1. Schematic of the laser system used to generate IR. BS represents a dichroic beam splitter, and PBC represents a polarizing beam combiner.

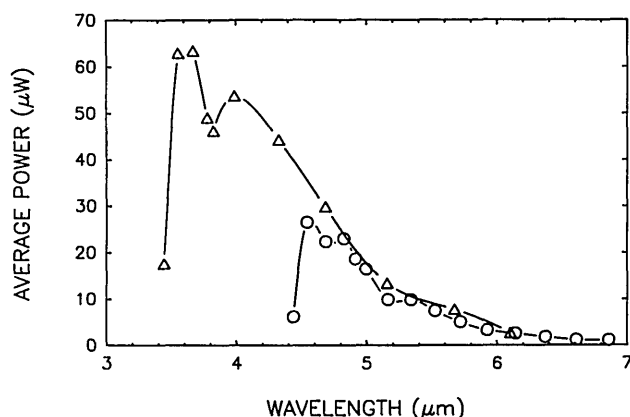


Fig. 2. Average IR output power as a function of IR wavelength. The curve from 3.4 to 6.2 μm was taken by using LDS 821 dye, and the curve from 4.4 to 7.0 μm was taken by using LDS 867 dye. Note that by using a different output coupler it is possible to extend the tuning range as far as 9.14 μm to the red (see text).

that is given by $\omega_0/2^{1/2} = 42.4 \mu\text{m}$. The confocal parameters inside the AgGaS_2 for the 1.06- μm radiation (5.5 cm) and for the 5- μm radiation (5.5 mm) were both considerably longer than the crystal length. In order to tune the IR output, we varied the dye laser frequency and the crystal phase-matching angle simultaneously.

In Fig. 2 we show the IR output power versus wavelength. The tuning range with LDS 821 dye was 3.4–6.2 μm , and with LDS 867 dye it was 4.4–7.0 μm . The IR power was linearly proportional to the dye laser output, and the wavelength range was limited by the dye laser range. We used two additional output couplers with the LDS 867 dye to achieve the ranges 3.8–6.15 μm and 5.2–9.14 μm . The IR power was measured with a commercial liquid-nitrogen-cooled HgCdTe detector–pre-amplifier system. The relative wavelength sensitivity of the device was calibrated by the manufacturer and is included in the data presented in Fig. 2. The calibration was performed for uniform illumination over the entire diode. Because we focused the light into the detector, our measured signals are 10% higher than would be predicted by the manufacturer and possess an inherent uncertainty of $\pm 10\%$, which is consistent with the overall 20% variation of signal intensity as the focused beam is scanned over the detector area.

The phase-matching curve is shown in Fig. 3, where the vertical axis is the internal crystal angle with respect to the optic axis. The variation of the incident angle with respect to the crystal surface normal was considerably larger because the index of refraction of AgGaS_2 is ~ 2.45 . The solid curve is the phase-matching angle predicted with the Sellmeier equation from Ref. 18. The agreement in shape is good, but the measured angles are 1.5° lower than predicted. Because the orientation of the crystal was verified to be within $\pm 0.5^\circ$ by the supplier (Cleveland Crystals), we believe that the offset indicates that the indices of the new commercial material are slightly different from those of the material measured in 1971 by Boyd *et al.*¹²

In experiments that require wavelength tuning over a limited range it is often useful to vary the dye laser output frequency while holding the crystal angle constant. This technique minimizes translation of the IR beam in subsequent portions of the experimental apparatus. In Fig. 4 we show the IR power as a function of the frequency at a fixed crystal angle. The FWHM of this curve is 36 cm^{-1} . The dashed curve shows the predicted relation $I(\Delta k) \sim [\sin(\Delta k L/2)/(\Delta k L/2)]^2$, where the phase-mismatch Δk is derived from the Sellmeier equation of Ref. 18 with the appropriate offset (as noted above) and

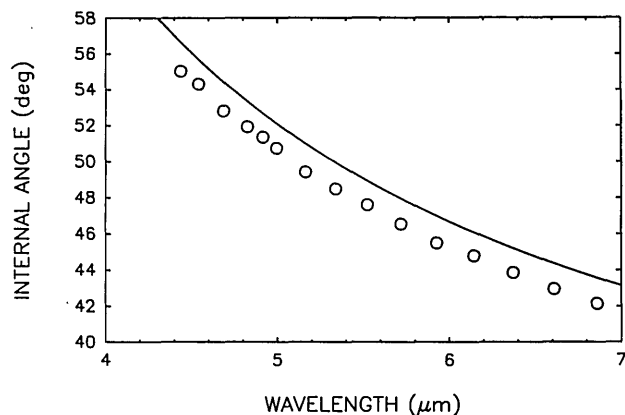


Fig. 3. Variation of AgGaS_2 phase-matching angle with respect to IR wavelength. Experimental data are represented by open circles. The solid curve is obtained theoretically with the Sellmeier equation¹⁸ and index of refraction data from Ref. 12.

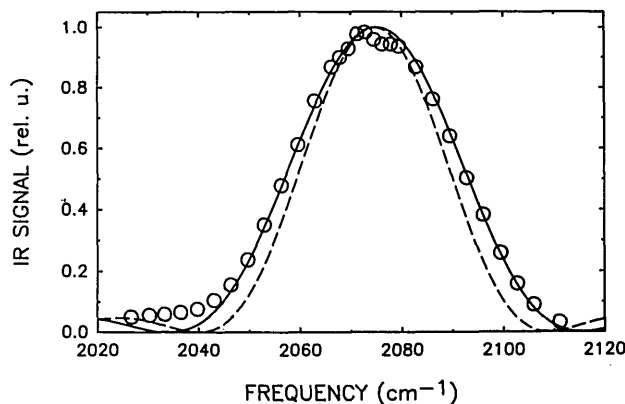


Fig. 4. IR average power as a function of wavelength for a fixed crystal orientation. Experimental data are open circles. Solid (dashed) curve is a fit to theory for an interaction length of 1.6 mm (1.4 mm).

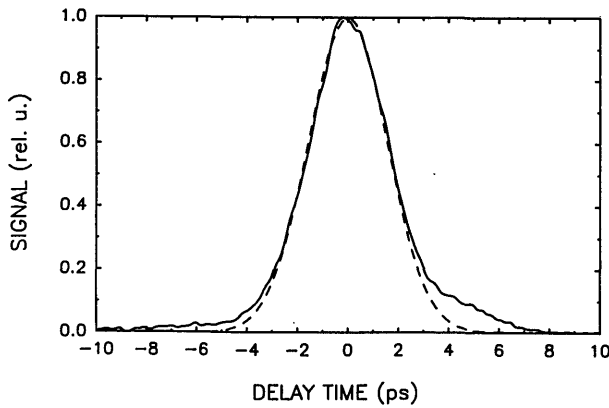


Fig. 5. Cross-correlation between IR output pulse at 5 μm and the frequency-doubled compressed YAG pulse ($\lambda = 0.532 \mu\text{m}$). The dashed curve represents the best Gaussian fit to the pulse shape.

L is the crystal length, 1.65 mm. This prediction does not fit the data so well as the solid curve, which is fitted with the same relation but with $L = 1.4$ mm. This result may be caused by a combination of walk-off, which limits the effective length of interaction, and the tight focus, which provides a fairly large distribution of output angles. The birefringent walk-off affects only the dye laser wavelength. The walk-off angle (θ_w) varies from approximately 1.1° to 1.24° for dye laser wavelengths from 785 to 984 nm, which permits tuning from 3 to 13 μm . For 5- μm generation the walk-off angle is 1.2° , which limits the effective length to

$$L_{\text{eff}} = \frac{\omega_0}{\sin \theta_w} \frac{2}{\pi^{1/2}} \text{erf} \left[L \left(\frac{\sin \theta_w}{\omega_0} \right) \right] = 1.49 \text{ mm}. \quad (1)$$

The tight focus of the 5- μm output beam may make the distribution of angles large enough that the maximum is never as large as one might predict for plane waves. This result is also consistent with the absence of clean zeros in the data when $\Delta kL/2 = \pi$. On the other hand, the large confocal parameter for the input beams gives an input acceptance angle $\pm 0.32^\circ$ for half-maximum intensity.

The IR pulse duration was measured by cross-correlating it with the frequency-doubled compressed YAG pulse at 532 nm by noncollinear sum-frequency generation in LiIO_3 . All pulses were assumed to be Gaussian, e.g., $I(t) = \exp(-2t^2/\tau^2)$. The central portion of the compressed 532-nm pulse autocorrelation was well fitted with $\tau_{0.532\mu\text{m}} = 2.24$ ps. The cross-correlation with the 5- μm pulse is shown in Fig. 5. The deconvolution of this shape yields $\tau_{5\mu\text{m}} = 2.15 \pm 0.1$ ps. Separate autocorrelations of the 1.06- and 0.87- μm pulses were fitted with $\tau_{1.06\mu\text{m}} = 3.17$ ps and $\tau_{0.87\mu\text{m}} = 2.54$ ps, and the difference-frequency output should have $\tau_{5\mu\text{m}} = (\tau_{1.06\mu\text{m}}^2 + \tau_{0.87\mu\text{m}}^2)^{1/2} = 2.0$ ps. Here we note that for Gaussian pulse shapes τ is related to the measured FWHM pulse duration (Δt) by $\Delta t = (2 \ln 2)^{1/2} \tau$. Furthermore, although the YAG pulse is never truly Gaussian, we continue to use the Gaussian forms for calculational simplicity. The observed pulse broadening is probably caused by group-velocity dispersion between n_o of the IR and $n_e(\theta)$ of the dye laser. The difference in transit time, $\Delta\tau$, of the pulses through the

crystal is $(5 \text{ ps/cm})L$. For our 1.65-mm crystal, $\Delta\tau$ is 0.825 ps, which, if convoluted with the expected pulse width because of straight mixing, gives $\tau_{5\mu\text{m}} = 2.16$ ps, in agreement with the measured value. Additional pulse broadening caused by spatial walk-off is negligible, since the effective length is shortened to only 1.49 mm. The slight wings in the cross-correlation function arise because the compressed 0.532- μm pulse has a pedestal.

We also measured the frequency FWHM bandwidths $\Delta\nu_{\text{FWHM}}$ to be 3.57 cm^{-1} for the 878-nm dye laser, 9.7 cm^{-1} for the compressed 1.06- μm pulse, and 6.6 cm^{-1} for the 5- μm pulse. We estimate the effective bandwidth of the compressed 1.06- μm pulse to be 6.4 cm^{-1} during the 3.0-ps FWHM of the 878-nm pulse. This estimate is obtained by assuming that the 1.06- μm pulse entering the fiber compressor has a hyperbolic-secant-squared temporal shape and that the fiber chirp is due only to self-phase modulation because the fiber is too short to contribute group-velocity dispersion. The convolution of 6.4 and 3.57 cm^{-1} is 7.3 cm^{-1} , which is in approximate agreement with the 6.6 cm^{-1} measured bandwidth of the 5- μm pulse. Despite the probable chirp on the compressed YAG pulse, it has a time-bandwidth product of 0.53, which is remarkably close to the transform limit for Gaussian pulses of 0.44.

The observed output power allows us to determine that the AgGaS_2 nonlinear coefficient d_{36} is $1.4 \times 10^{-7} \pm 20\%$ esu. Here we use the formula for a Gaussian beam focus in the regime for which the crystal length is much less than the confocal parameters²⁰:

$$\frac{S(\omega_1)}{S(\omega_2)S(\omega_3)} = \frac{(64\pi^2)\omega_1^2}{c^3 n_1 n_2 n_3} |2d_{36} \sin \theta_m|^2 \times \frac{L_{\text{eff}}^2}{W_1^2 + W_2^2} \frac{\tau_3}{(\pi/2)^{1/2} \tau_1 \tau_2} F, \quad (2)$$

where subscripts 1, 2, and 3 refer to the radiation at IR, 1.06- μm , and 0.88- μm wavelengths. $S(\omega_i)$ denotes the energy per pulse at the frequency ω_i in ergs, τ_i denotes the Gaussian pulse widths measured above, W_i is the Gaussian radius of the incident beams (60 μm), and n_i is the index of refraction at frequency ω_i , which is taken to be 2.45 here. $F = 0.83$ is the Fresnel loss. The measured average powers were 18 μW at 5 μm , 50 mW at 878 nm, and 235 mW at 1.06 μm . We use the effective length 1.4 mm in accordance with the fit to Fig. 4. Here we assume that only $50 \pm 10\%$ of the energy in the compressed pulse resides in the temporally short central portion of the pulse. This is consistent with autocorrelation measurements that indicate that the wings are symmetric, are 1/8 the peak intensity, and are twice the duration of the central pulse. We also assume that the beams are Gaussian, both spatially and temporally (which could lead to $\sim 20\%$ errors). Our result agrees with literature values but is half as large as the value given by Boyd *et al.*¹² The nonlinear coefficients for doubling 10.6 μm are 18×10^{-12} and 56×10^{-12} m/V in Refs. 12 and 13, respectively. Using Miller's constant- Δ condition,¹² d_{36} for our 5- μm generation case is 24×10^{-12} and 75×10^{-12} m/V, or 5.7×10^{-8} and 1.8×10^{-7} esu. Our value of 2.2×10^{-8} esu is closer to the value 5.7×10^{-8} esu.

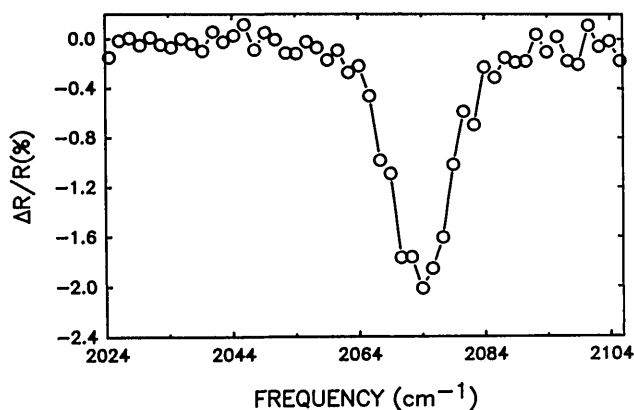


Fig. 6. Results of a single 1-min linear absorption scan that uses the source to probe the atop resonance of CO adsorbed on Cu[111] at 110 K in ultrahigh vacuum.

CURRENT LIMITATIONS AND IMPROVEMENTS

The apparatus we describe offers the user a tunable, high-repetition-rate picosecond probe pulse. We recently used the probe to measure the linear absorption of a monolayer of CO adsorbed on Cu[111] in ultrahigh vacuum.²¹ Results of a single 1-min linear reflection measurement are shown in Fig. 6. The scan reveals a 2% amplitude variation with a 10:1 signal-to-noise ratio. The measured bandwidth of the IR line is 11.3 cm^{-1} . Since the bandwidth of our IR source is 6.6 cm^{-1} , we predict that the line has a natural width of 9.2 cm^{-1} . This prediction is consistent with literature values of 11 (Ref. 22) and 9 cm^{-1} .²³ In future pump-probe experiments pump modulation at 200 kHz will enable us to see changes as small as 10^{-6} . In addition, a number of other improvements can further enhance the utility of this tool.

The largest intensity fluctuations present in the Nd:YAG laser occur on the 100-ms time scale and are $\sim 2\%$ of the average output power. Unfortunately these fluctuations are impressed on the dye laser output and, along with pulse duration fluctuations, are amplified in the compressed $1.06\text{-}\mu\text{m}$ output. This amplification results in $\sim 10\%$ IR intensity fluctuations on slow time scales. Under these circumstances linear spectroscopy is difficult to carry out without some type of normalization procedure. Active stabilization techniques offer the possibility of significantly decreasing the total fluctuations. A number of noise eater schemes are currently in use. Typically these schemes monitor the doubled light and then vary the rf drive power of an acousto-optic modulator that is located just after the Nd:YAG laser to compensate for these changes. Fluctuations as low as 1×10^{-5} in the parent laser (below 1 kHz) have been reported.²⁴ In this case we expect our IR intensity to fluctuate at less than the 1% level.

The temporal jitter between the compressed $1.06\text{-}\mu\text{m}$ light pulses and the dye laser pulses presents another limitation on the time resolution of this system²⁵ even if the pulses can be shortened. We measured this jitter by cross-correlation and found it to be less than 1 ps. The most direct way to reduce this problem is to stabilize the amplitude of the Nd:YAG laser, since the timing of the dye laser pulse depends strongly on the degree to which

the dye laser is above threshold and hence on the pump pulse energy.

Two obvious additional improvements to the system would be to extend the tuning range further into the IR and to shorten the pulses. To extend the tuning range, it is necessary to try new dye mixtures and various dye laser optics in order to shift the cavity Q further to the red. The AgGaS₂ phase matchability and absorption losses do not become limitations until λ_{IR} is $\sim 12 \mu\text{m}$. Shortening the dye pulses to $\sim 500 \text{ fs}$ is possible by introducing a single-plate birefringent filter or saturable absorbers into the dye laser cavity. However, group-velocity dispersion would require reduction of the length of the crystal to $\sim 300 \mu\text{m}$ to keep the IR pulse widths temporally short.

In conclusion, we have described an apparatus that possesses broad tunability in the mid-IR spectral region as well as a high repetition rate and picosecond temporal resolution. The apparatus is relatively easy to set up and offers a probe that is compatible with lock-in detection techniques.

*Present address, Department of Physics, University of Pennsylvania, Philadelphia, Pennsylvania 19104.

REFERENCES

1. See, for example, D. A. King, N. V. Richardson, and S. Holway, eds., *Vibrations at Surfaces 1985* (Elsevier, Amsterdam, 1986).
2. T. Elsaesser, H. Lobentanzer, and A. Seilmeier, *Opt. Commun.* **52**, 355 (1985).
3. A. Seilmeier, K. Spanner, A. Laubereau, and W. Kaiser, *Opt. Commun.* **24**, 237 (1978).
4. T. Elsaesser, A. Seilmeier, W. Kaiser, P. Koidl, and G. Brandt, *Appl. Phys. Lett.* **44**, 383 (1984).
5. T. M. Jedju and L. Rothberg, *Appl. Opt.* **26**, 2877 (1987).
6. D. S. Moore and S. C. Schmidt, *Opt. Lett.* **12**, 480 (1987).
7. J. H. Glowina, J. Misewich, and P. P. Sorokin, *Opt. Lett.* **12**, 19 (1987).
8. M. Berg, A. L. Harris, J. K. Brown, and C. B. Harris, *Opt. Lett.* **9**, 50 (1984).
9. J. N. Moore, P. A. Hansen, and R. M. Hochstrasser, *Chem. Phys. Lett.* **138**, 110 (1987); P. A. Hansen, J. N. Moore, and R. M. Hochstrasser, *Chem. Phys.* **131**, 49 (1989); P. Anfinrud, C. Han, P. A. Hansen, J. N. Moore, and R. M. Hochstrasser, in *Ultrafast Phenomena VI*, T. Yajima, K. Yoshihara, C. B. Harris, and S. Shionoya, eds. (Springer-Verlag, Berlin, 1988), p. 442.
10. See Y. R. Shen, ed., *Nonlinear Infrared Generation* (Springer-Verlag, New York, 1977).
11. A. G. Yodh, H. W. K. Tom, and G. D. Aumiller, *Conference on Lasers and Electro-Optics*, Vol. 7 of 1988 OSA Technical Digest Series (Optical Society of America, Washington, D.C., 1988), p. 408.
12. G. D. Boyd, H. Kasper, and J. H. McFee, *IEEE J. Quantum Electron.* **QE-7**, 563 (1971).
13. P. J. Kupecek, C. A. Schwartz, and D. S. Chemla, *IEEE J. Quantum Electron.* **QE-10**, 540 (1974).
14. P. C. Becker, D. Gershoni, and A. Prosser, in *Ultrafast Phenomena VII*, C. Harris, E. Ippen, G. Mourou, and A. Zewail, eds. (Springer-Verlag, Berlin, 1990), p. 81; T. Elsaesser and M. C. Nuss, in *Ultrafast Phenomena VII*, C. Harris, E. Ippen, G. Mourou, and A. Zewail, eds. (Springer-Verlag, Berlin, 1990), p. 85.
15. I. S. Ruddock, R. Illingworth, and L. Reekie, *Opt. Quantum Electron. (UK)* **16**, 87 (1984).
16. H. Vanherzele, *Appl. Opt.* **29**, 2246 (1990).
17. For a review of stimulated electronic Raman scattering in gases, see J. J. Wynne and P. P. Sorokin, in *Nonlinear Infrared Generation*, Y. R. Shen, ed. (Springer-Verlag, Berlin, 1977), p. 159.

18. See, for example, Y. X. Fan and R. L. Byer, in *New Lasers for Analytical & Industrial Chemistry*, A. F. Bernhardt, ed., Proc. Soc. Photo-Opt. Instrum. Eng. **461**, 27 (1984), and references therein.
19. See, for example, H. Nakatsuka, D. Grischkowsky, and A. C. Balant, Phys. Rev. Lett. **47**, 910 (1981); C. V. Shank, R. L. Fork, R. Yen, R. H. Stolen, and W. J. Tomlinson, Opt. Lett. **8**, 289 (1983); W. J. Tomlinson, R. H. Stolen, and C. V. Shank, J. Opt. Soc. Am B **1**, 139 (1984).
20. Y. R. Shen, *The Principles of Nonlinear Optics* (Wiley, New York 1984).
21. A. G. Yodh and H. W. K. Tom, presented at the Fourth International Conference of Time-Resolved Vibrational Spectroscopy, Princeton, N.J., 1989.
22. P. Hollins and J. Pritchard, Surf. Sci. **89**, 486 (1979).
23. B. E. Hayden, K. Dretzschmar, and A. Bradshaw, Surf. Sci. **155**, 533 (1985).
24. L. F. Mollenauer, AT&T Bell Laboratories, Holmdel, N. J. 07733 (personal communication, July 1988).
25. U. Siegner, G. Noll, and E. O. Gobel, Appl. Phys. B **48**, 21 (1989).